Desalination and Water Treatment
www.deswater.com
doi: 10.1080/19443994.2014.982193

57 (2016) 2152–2158
January

Taylor & Francis
Taylor & Francis Group

Molecular simulations and critical pH studies for the interactions between 2-phosphonobutane-1,2,4-tricarboxylic acid and calcite surfaces in circular cooling water systems

Jiaomei Jiang[a], Jianping Zhao[b,*], Yanhua Xu[a]

[a]*Jiangsu Key Laboratory of Industrial Water-Conservation & Emission Reduction, College of Environment, Nanjing Tech University, Nanjing, Jiangsu 210009, China, Tel. +86 25 5813 9654; email: jiaomeijiang@163.com (J. Jiang), Tel. +86 25 5813 9649; email: xuyh@njtech.edu.cn (Y. Xu)*
[b]*School of Mechanical and Power Engineering, Nanjing Tech University, Nanjing, Jiangsu 210009, China, Tel. +86 25 5813 9360; email: jpzhao71@163.com*

Received 19 March 2014; Accepted 24 October 2014

ABSTRACT

The adsorption of 2-phosphonobutane-1,2,4-tricarboxylic acid (PBTC) on calcite surfaces (1 $\bar{1}$ 0), (1 0 2), (1 0 4), (1 1 3), (2 0 2) was studied by molecular simulation. The phosphoric acid and carboxylic acid functional groups energetically interacted with the faces and preferentially occupied the carbonate ion sites by chemisorption, which is in agreement with the critical pH experiments. The strength of adsorption followed the order of (1 $\bar{1}$ 0) > (1 1 3) > (1 0 2) > (2 0 2) > (1 0 4). The binding energy gradually decreased with increasing temperature. The relationship between the critical pH and the adsorbed $PBTC^{2-}$ configuration indicates that the adsorbed inhibitor configuration plays an important role in inhibitor efficiency.

Keywords: Computer simulation; Preferential adsorption site; Scale inhibitor; Calcite

1. Introduction

Chemical crystallization is one of the important causes of scale formation in cooling water systems. The use of phosphonates as the scale and corrosion inhibitors is an effective method for preventing mineral scale and corrosion [1,2]. Previous studies have shown that scale inhibitors can broaden the width of a metastable zone [3], increase the induction time, inhibit crystal growth [4], and change the crystal morphology [5,6]. The fundamentals of scale inhibition mechanism are inadequately understood [7]. Experimental and experience extrapolation methods are the leading methods for the performance evaluation of new scale inhibitors, which commonly waste time, manpower, and material resources [8]. More investigations are needed to understand the scale inhibition process at the molecular level. Molecular simulation approaches are useful for investigating inhibition mechanism.

Calcite is the predominant component of scales deposited in cooling water systems [9–14]. The critical pH of calcite increases by adding inhibitors. This increases the width of calcite crystallization metastable zone. Thus, the critical pH of calcite indicates the inhibition effect [3].

In this study, the width of calcite crystallization metastable zone was investigated by determining the critical pH of the crystallization system [15–17] in a

*Corresponding author.

jacketed crystallizer at different temperatures. Moreover, molecular simulation was used to investigate the adsorption behavior of 2-phosphonobutane-1,2,4-tricarboxylic acid (PBTC) on calcite surfaces. The adsorption of an inhibitor on calcite surface affects the crystallization of calcite. Therefore, it is important to investigate the relationship between the critical pH and the properties of adsorbed $PBTC^{2-}$ properties on calcite surfaces.

2. Effect of PBTC on calcite crystallization metastable zone

2.1. Experimental procedures

When a NaOH solution was added, the pH of the experimental system increased. When calcite precipitated, the pH of the experimental system decreased. Fig. 1 shows the inflection point known as critical pH.

Fig. 2 shows the schematic drawing of the experimental apparatus. The stable experimental solution was prepared by mixing calcium chloride (6.0 mM) and sodium bicarbonate (13.8 mM) solutions using a magnetic stirrer at a constant speed. A metering pump was used for pumping 0.1 M NaOH solution at a speed of 0.05 mL min^{-1}. A pH sensor was used to measure the solution pH during $CaCO_3$ crystallization process [3].

2.2. Results and discussion

The critical pH experiments were performed at five temperatures. To qualitatively analyze the metastable zone, the pH values of the mixed solutions were measured after the addition of PBTC at different concentrations (0.001–0.005 mM).

Fig. 3 shows that the pH values slowly increased when 0.004 mM concentration of PBTC was used. This indicates that the inhibition of calcite growth with 0.004 mM PBTC was successful at five temperatures. As shown in Fig. 4, the calcite metastable zone width narrowed with increasing temperature.

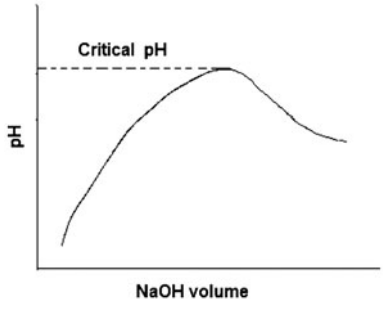

Fig. 1. pH curve.

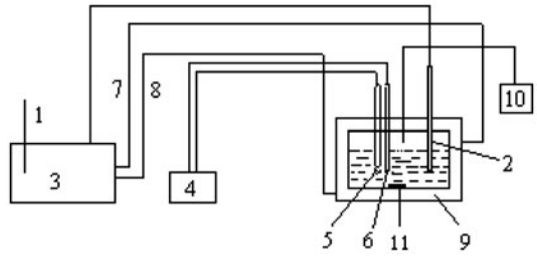

Fig. 2. Schematic of experimental setup. 1, Thermometer; 2, temperature probe; 3, super constant temperature water bathing; 4, acidometer; 5, glass electrode; 6, reference electrode; 7, outlet line of crystallizer; 8, inlet line of crystallizer; 9, jacketed crystallizer; 10, metering pump; 11, magnetic stirrer.

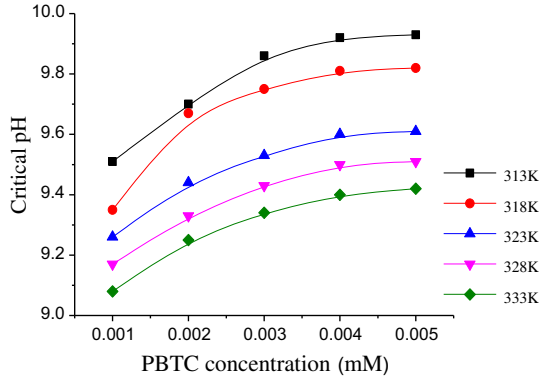

Fig. 3. Critical pH with different concentrations of PBTC at five temperatures.

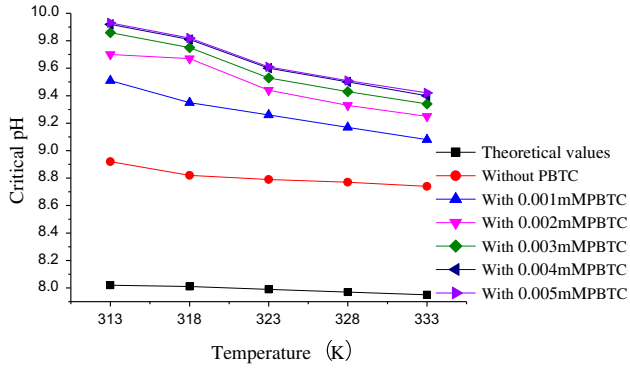

Fig. 4. Calcite metastable zone with different concentrations of PBTC at five temperatures.

3. Molecular simulations of the interactions between PBTC and calcite surfaces

3.1. Theoretical models and methods

The pH value is usually controlled stably from 8.0 to 9.0 in cooling water systems. At these pH values,

Table 1
Simulation of box lattice parameters

	(1 $\bar{1}$ 0)	(1 0 2)	(1 0 4)	(1 1 3)	(2 0 2)
a (Å)	49.90	53.37	64.76	51.85	51.00
b (Å)	51.18	49.90	49.90	51.00	49.90
c (Å)	72.38	69.97	63.70	61.45	60.53
α (°)	90	90	90	90	90
β (°)	90	90	90	90	90
γ (°)	90	90	90	103	67

PBTC exists as an anion. In this study, $PBTC^{2-}$ ions were adsorbed on the calcite surfaces [18].

The molecular simulation studies were performed using the COMPASS force field [19,20], which enabled the accurate and simultaneous prediction of chemical properties (structure, conformation, vibration, etc.) and condensed-phase properties (equation of state, cohesive energies, etc.) for diverse chemical systems. This is the first high-quality force field combining the parameters of organics and inorganics.

The space group of calcite is R-3C, and its lattice parameters are $a = b = 4.99$ Å, $c = 17.06$ Å, $\alpha = \beta = 90.0°$, and $\gamma = 120.0°$. The (1 $\bar{1}$ 0), (1 0 2), (1 0 4), (1 1 3), and (2 0 2) [21–24] surfaces were cut and optimized. The simulation box lattice parameters are shown in Table 1. First, we simulated the characteristics of $PBTC^{2-}$ on each calcite face to determine the easily adsorbing faces and optimal binding sites by the Monte Carlo sampling and simulated annealing calculation methods. The Monte Carlo method randomly sampled the configurations of $PBTC^{2-}$ and placed each configuration on the calcite surfaces by conformer, rotation, and translation. The conformer, translation, and rotation steps were used with a probability of 0.33 each. The simulated annealing method used Monte Carlo sampling when the system temperature gradually decreased. This progress was repeated several times to identify further local energy minima. To obtain good statistics, 10 simulated annealing cycles decreased the temperature from 1,000 to 313, 318, 323, 328, and 333 K were performed (a total 50,000 steps per cycle). Later, we calculated the property parameters of the adsorbed $PBTC^{2-}$ configurations by DMol^3. In this study, the dielectric constant (ε) was set at 78.0, and the temperatures were set at 313, 318, 323, 328, and 333 K according to the actual circular water environment. The simulation details are shown in Table 2.

The strength of the interactions of the surface with the adsorbate is shown by the binding energy, calculated according to Eqs. (1) and (2) as follows:

$$\Delta E = E_t - (E_s + E_i) \quad (1)$$

$$E_b = -\Delta E \quad (2)$$

where E_t is the total energy of the surface and inhibitor, E_s is the energy of the surface without the inhibitor, and E_i is the energy of the inhibitor without the surface.

3.2. Results and discussion

3.2.1. Adsorption of $PBTC^{2-}$ on calcite faces

According to the periodic bond chains (PBC) theory (the model as shown in Fig. 5), the crystal growth surfaces were grouped into three types, namely, flat face, step face, and kink face [25]. Flat faces are the most

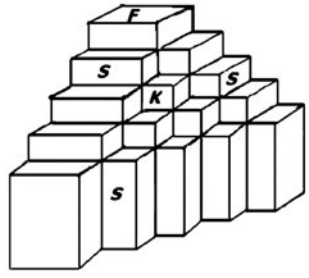

Fig. 5. Model of PBC theory: F, flat face; S, step face; and K, kink face.

Table 2
Simulation details

Simulation parameters	Option	Simulation parameters	Option
Calculation method	Simulated annealing	Electrostatic	Group based
Sampling method	Monte Carlo	Van der Waals	Atom based
Force field	COMPASS	Cutoff distance	9.5 Å
Maximum temperature	1,000 K	Ensemble	NVT
Final temperatures	313, 318, 323, 328, and 333 K	Thermostat	Nosé
Probability	0.33	Q ratio	2.0

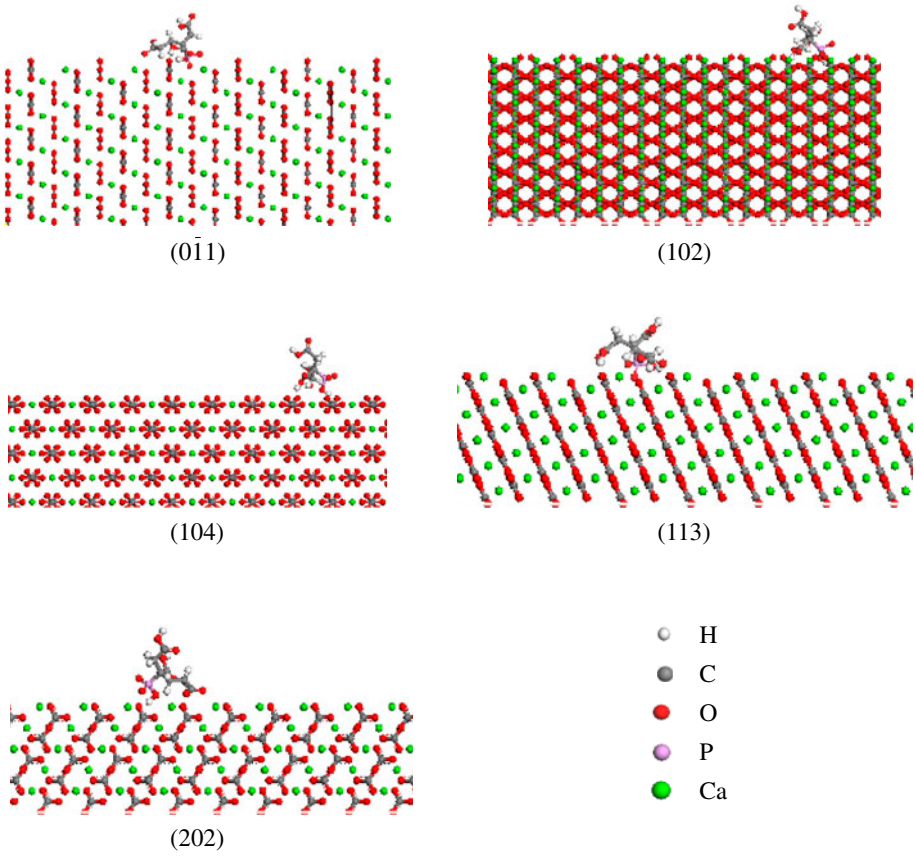

Fig. 6. Most suitable configurations and preferential adsorption sites of $PBTC^{2-}$ ions on calcite surfaces.

stable surfaces because of the slowest growth rate. This indicates that the probability of the adsorption of organic additives on flat faces is very remarkable.

Fig. 6 shows the adsorption of PBTC on calcite faces, (1 $\bar{1}$ 0), (1 0 2), (1 0 4), (1 1 3), and (2 0 2). Clearly, the carbonate and phosphonate groups in PBTC were close to the crystal surfaces. Fig. 7 is shown in the side view to clearly indicate how the carbonate and phosphonate groups are close to the surfaces. The oxygen atoms of the carbonate and phosphonate groups interact with calcium ions and preferentially occupy the carbonate ion sites on the calcite faces, thus increasing the interactions and steric hindrance and avoid crystal aggregation. The equilibrium in water: $HCO_3^- \Leftrightarrow CO_3^{2-} + H^+$ is difficult to move to the right. This explains why the critical pH value increased after adding the inhibitor in circular cooling water system.

The interaction energies of all the surface systems at 323 K are listed in Table 3. The interaction energies of all the systems are negative, indicating that the combination of $PBTC^{2-}$ ions with the calcite surfaces is exothermic. Furthermore, the conventional physisorption energy is generally 40 kJ mol^{-1} or so. The conventional chemisorption energy is typically more than 80 kJ mol^{-1} [26,27]. The values of the interaction energies are much higher than the conventional adsorption energy, indicating that the adsorption is chemisorption. Chemisorption is significantly different from physisorption in that it is highly selective and involves monolayer adsorption. This can be confirmed by the experimental results.

As shown in Table 3, the sequence of the binding energies of the five surfaces with $PBTC^{2-}$ is (1 $\bar{1}$ 0) > (1 1 3) > (1 0 2) > (2 0 2) > (1 0 4). In Fig. 7, the distance of the oxygen atoms in $PBTC^{2-}$ and the nearest calcium ions on calcite surface is slightly longer than the electrovalent bond length of O–Ca. This indicates the electrovalent bonds formed between $PBTC^{2-}$ and calcium ions. [8]. Fig. 7 shows that the numbers of O–Ca bonds on (1 $\bar{1}$ 0) and (1 1 3) are more than those on the other surfaces. The numbers of O–Ca bonds on (104) are less than those on the other surfaces. This indicates that the strength of binding energy is

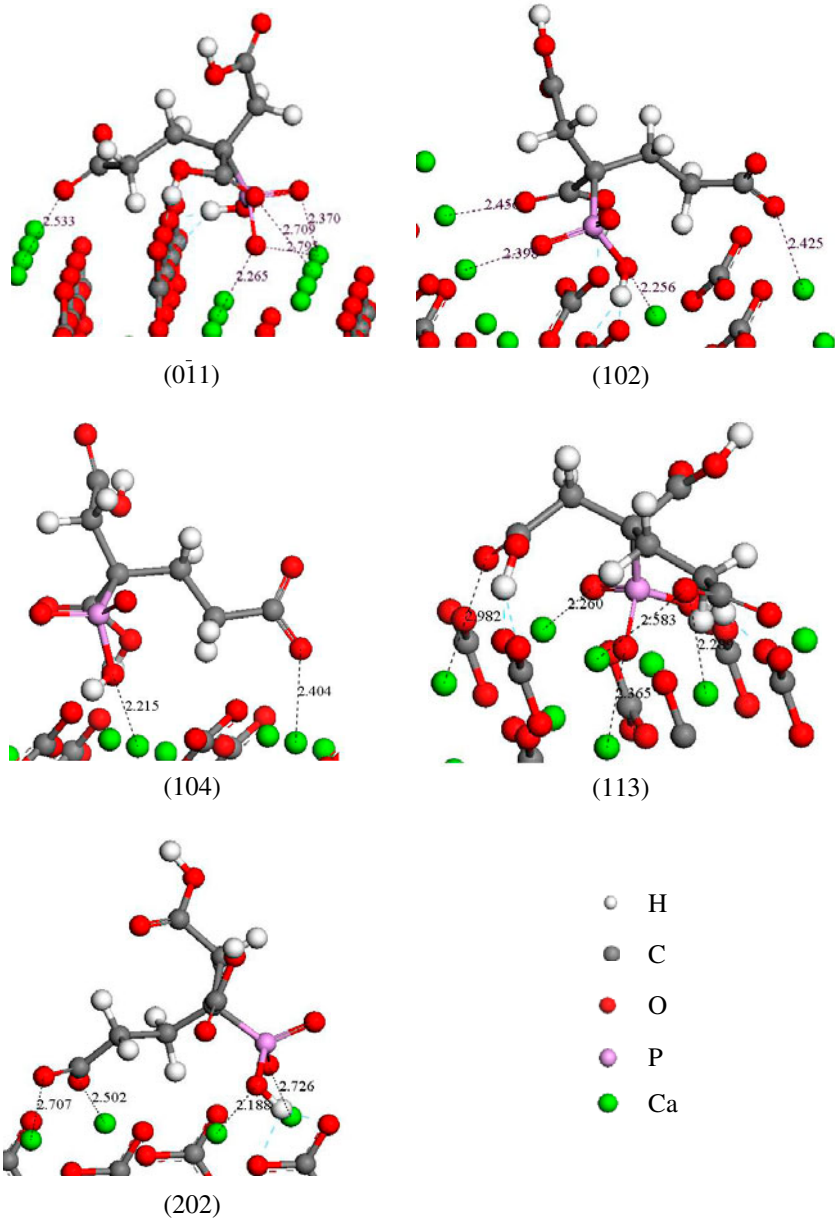

Fig. 7. O–Ca bonds of the oxygen atoms in $PBTC^{2-}$ ions and the nearest calcium ions on calcite surface.

Table 3
Interaction energies (kcal mol^{-1}) between $PBTC^{2-}$ ions and calcite surfaces

Surfaces	E_t	E_s	E_i	ΔE	E_b
(1 $\bar{1}$ 0)	−14627.81	−14322.68	−153.41	−151.72	151.72
(104)	−18399.26	−18197.23	−138.03	−64.00	64.00
(102)	−19542.98	−19264.16	−156.30	−122.52	122.52
(113)	−17208.2	−16909.23	−157.69	−141.28	141.28
(202)	−9553.37	−9311.13	−139.44	−102.80	102.80

Table 4
Effect of temperature (K) on the binding energies (kcal mol^{-1}) between $PBTC^{2-}$ ions and calcite surface

Surfaces	313	318	323	328	333
($\bar{1}$ 1 0)	166.56	154.20	151.72	151.29	132.66
(104)	65.06	64.35	64.00	58.20	57.39
(102)	136.35	133.31	122.52	122.34	115.40
(113)	141.37	141.28	141.28	127.94	111.55
(202)	105.83	102.82	102.80	98.61	97.01

Table 5
Property parameters of different $PBTC^{2-}$ ion configurations

T (K)	pH	μ (e Å)	E_H (kcal mol^{-1})	E_L (kcal mol^{-1})
313	9.93	2.1130	−0.2615	−0.2598
318	9.82	2.6548	−0.2827	−0.2780
323	9.61	2.0012	−0.2748	−0.1194
328	9.51	2.0591	−0.2682	−0.0965
333	9.42	2.2135	−0.2701	−0.0946

dominated by the numbers of the O–Ca bonds. The combinations of $PBTC^{2-}$ ions with the (1 $\bar{1}$ 0) surface are easier than those with the others. It can significantly affect the growth of the (1 $\bar{1}$ 0) surface.

3.2.2. Effect of temperature on the binding energies between $PBTC^{2-}$ ions and calcite faces

To determine the effect of temperature on the binding energies between $PBTC^{2-}$ ions and the calcite surfaces, the interactions were simulated at different temperatures ranging from 313 to 333 K, and the binding energies are shown in Table 4.

As shown in Table 4 and Fig. 4, as the temperature increased, the binding energy and critical pH gradually decreased. At the same temperature, the sequence of the binding energies of the five surfaces is similar as follows: (1 $\bar{1}$ 0) > (1 1 3) > (1 0 2) > (2 0 2) > (1 0 4).

3.2.3. Relationship between the critical pH and adsorbed $PBTC^{2-}$ configuration

The adsorption of $PBTC^{2-}$ ions on calcite surfaces affects the inhibition efficiency. To investigate the relationship between the critical pH (pH_c) and the adsorbed $PBTC^{2-}$ configuration, the properties of adsorbed $PBTC^{2-}$ ions on (1 0 4) at different temperatures were calculated by DMol^3, as listed in Table 5.

E_H (the highest occupied molecular orbital energy) is often associated with the electron-donating ability of the molecule. High values of E_H probably indicate a tendency to donate electrons to appropriate acceptors. At the five temperatures, the E_H values are similar.

E_L (the lowest unoccupied molecular orbital energy) indicates the ability to accept electrons [28]. At 318 K, E_L is the lowest. The dipole moment μ indicates the electronic distribution in a molecule [29]. At 318 K, μ has the highest value, and the polarity of $PBTC^{2-}$ ions is strong. To investigate the relationship between the critical pH and the configuration properties, multiple linear regressions were applied. The result is shown as follows:

$$pH_c = 9.937 - 0.343\mu - 2.816E_L \quad (R^2 = 0.9836) \tag{3}$$

This clearly indicates that the critical pH correlated well with the μ and E_L of the adsorbed $PBTC^{2-}$ ions. This is very helpful to understand the mechanism of the interactions between the inhibitor and calcite surfaces and to design novel inhibitors.

4. Conclusions

The pH values during the calcite crystallization process were determined. The inhibitor PBTC improved the calcite critical pH value and widened the metastable zone of calcite. At the five studied temperatures, the calcite metastable zone was the widest when the PBTC concentration was 0.004 mM. The calcite metastable zone width narrowed with increasing temperature.

Molecular simulations were employed to study the adsorption of PBTC on calcite surfaces. The results indicate that the phosphoric acid and carboxylic acid groups energetically interacted with the faces and preferentially occupied the carbonate ion sites by chemisorptions, in agreement with the results of the critical pH experiments. The sequence of the binding energies of the five surfaces with $PBTC^{2-}$ ions is as follows: (1 $\bar{1}$ 0) > (1 1 3) > (1 0 2) > (2 0 2) > (1 0 4). The strength of the binding energy was dominated by the numbers of the O–Ca bonds. The binding energy gradually decreased with increasing temperature. The relationship between the critical pH and adsorbed $PBTC^{2-}$ ion configurations indicates that the inhibitor configurations play an important role in inhibitor efficiency. The future study will focus on the interactions of the calcite surfaces with PBTC in the presence of Cl^- and Mg^{2+} ions.

Acknowledgments

This work was supported by the Jiangsu Key Laboratory of Industrial Water-Conservation and Emission Reduction and Natural Science Foundation of Education Department, Jiangsu Province (No. 11KJA610001) titled "Mechanism and new control technology of corrosion and fouling organisms in nuclear power circulating seawater."

References

[1] B.R. Zhang, L. Zhang, F.T. Li, W. Hu, P.M. Hannam, Testing the formation of Ca–phosphonate precipitates and evaluating the anionic polymers as Ca–phosphonate precipitates and $CaCO_3$ scale inhibitor in simulated cooling water, Corros. Sci. 52 (2010) 3883–3890.

[2] Q.F. Yang, Y.Q. Liu, A.Z. Gu, J. Ding, Z. Shen, Investigation of calcium carbonate scaling inhibition and scale morphology by AFM, J. Colloid Interface Sci. 240 (2001) 608–621.

[3] J.M. Jiang, Y.H. Xu, New estimation of the dosage of scale inhibitor in the cooling water system, E-J. Chem. 8 (2011) 1881–1885.

[4] V. Tantayakom, T. Sreethawong, H.S. Fogler, Scale inhibition study by turbidity measurement, J. Colloid Interface Sci. 284 (2005) 57–65.

[5] C. Martos, B. Coto, J.L. Peña, R. Rodríguez, D. Merino-Garcia, G. Pastor, Effect of precipitation procedure and detection technique on particle size distribution of $CaCO_3$, J. Cryst. Growth 312 (2010) 2756–2763.

[6] Y. Tang, W. Yang, X. Yin, Y. Liu, P. Yin, J. Wang, Investigation of $CaCO_3$ scale inhibition by PAA ATMP and PAPEMP, Desalination 228 (2008) 55–60.

[7] S. He, A.T. Kan, M.B. Tomson, Inhibition of calcium carbonate precipitation in NaCl brines from 25 to 90°C, Appl. Geochem. 14 (1999) 17–25.

[8] W.Y. Shi, C. Ding, J.L. Yan, X.Y. Han, Z.M. Lv, W. Lei, M.Z. Xia, Molecular dynamics simulation for interaction of PESA and acrylic copolymers with calcite crystal surfaces, Desalination 291 (2012) 8–14.

[9] C. Wang, S. Li, T. Li, Calcium carbonate inhibition by a phosphonate-terminated poly(maleic-co-sulfonate) polymeric inhibitor, Desalination 249 (2010) 1–4.

[10] Q. Yang, Y. Liu, A. Gu, J. Ding, Z. Shen, Investigation of induction period and morphology of $CaCO_3$ fouling on heated surface, Chem. Eng. Sci. 57 (2002) 921–931.

[11] R. Ketrane, B. Saidani, O. Gil, L. Leleyter, F. Baraud, Efficiency of five scale inhibitors on calcium carbonate precipitation from hard water: Effect of temperature and concentration, Desalination 249 (2009) 1397–1404.

[12] N. Abdel-Aal, K. Sawada, Inhibition of adhesion and precipitation of $CaCO_3$ by aminopolyphosphonate, J. Cryst. Growth 256 (2003) 188–200.

[13] W.T. Kim, Y.I. Cho, A study of scale formation around air bubble attached on a heat-transfer surface, Int. Commun. Heat Mass Transfer 29 (2002) 1–14.

[14] A.L. Kavitha, T. Vasudevan, H.G. Prabu, Evaluation of synthesized antiscalants for cooling water system application, Desalination 268 (2011) 38–45.

[15] L.M. McGaughey, J.V. Matson, Prediction of the calcium carbonate saturation pH in cooling water, Water Res. 14 (1980) 1729–1735.

[16] I. Drela, P. Falewicz, S. Kuczkowska, New rapid test for evaluation of scale inhibitors, Water Res. 32 (1998) 3188–3191.

[17] L. Martens, K.P. Sa, Critical pH in cooling water, in: F. Colin, P. Quevauviller (Eds.), Monitoring of Water Quality: The Contribution of Advanced Technologies, Elsevier, Amsterdam, 1998, pp. 167–176.

[18] C.M. Pina, C.V. Putnis, U. Becker, S. Biswas, E.C. Carroll, D. Bosbach, A. Putnis, An atomic force microscopy and molecular simulations study of the inhibition of barite growth by phosphonates, Surf. Sci. 553 (2004) 61–74.

[19] A.Y. Musa, A.A.H. Kadhum, A.B. Mohamad, M.S. Takriff, M. Abu Bakar, Molecular dynamics and quantum chemical calculation studies on 4,4-dimethyl-3-thiosemicarbazide as corrosion inhibitor in 2.5 M H_2SO_4, Mater. Chem. Phys. 129 (2011) 660–665.

[20] M.K. Awad, M.R. Mustafa, M.M.A. Elnga, Computational simulation of the molecular structure of some triazoles as inhibitors for the corrosion of metal surface, J. Mol. Struct.: Theochem. 959 (2010) 66–74.

[21] H. Sun, COMPASS: An ab initio force-field optimized for condensed-phase applicationsoverview with details on alkane and benzene compounds, J. Phys. Chem. B 102 (1998) 7338–7364.

[22] B. Nowack, A.T. Stone, Adsorption of phosphonates onto the goethite–water interface, J. Colloid Interface Sci. 214 (1999) 20–30.

[23] M.M. Reddy, A.R. Hoch, Calcite crystal growth rate inhibition by polycarboxylic acids, J. Colloid Interface Sci. 235 (2001) 365–370.

[24] F. Manoli, J. Kanakis, P. Malkaj, E. Dalas, The effect of aminoacids on the crystal growth of calcium carbonate, J. Cryst. Growth 236 (2002) 363–370.

[25] P. Hartman, W.G. Perdok, On the relations between structure and morphology of crystals, Acta Crystallogr. 8 (1955) 49–52.

[26] H.Y. Erbil, Surface Chemistry of Solid and Liquid Interfaces, Blackwell, Oxford, 2006.

[27] A.W. Adamson, Physical Chemistry of Surfaces, Wiley-Interscience, New York, NY, 1997.

[28] I. Lukovits, K. Pálfi, I. Bakó, E. Kálmán, LKP model of the inhibition mechanism of thiourea compounds, Corrosion 53 (1997) 915–919.

[29] K.F. Khaled, Experimental, density function theory calculations and molecular dynamics simulations to investigate the adsorption of some thiourea derivatives on iron surface in nitric acid solutions, Appl. Surf. Sci. 256 (2010) 6753–6763.